PHYSICAL REVIEW D VOLUME 15, NUMBER 3 1 FEBRUARY 1977

Diffractive inelastic monopole transitions and the slope-mass relation in πN production*

P. M. Fishbane and J. V. Noble

Department of Physics, University of Virginia, Charlottesville, Virginia 22901

(Received 7 June 1976)

The t slope and peripheral structure of the cross sections $d^2\sigma/dt\,dm_{\pi N}$ for diffractive πN production can be understood as a coherent superposition of non-spin-flip ($\Delta l = 0$) inelastic two-body amplitudes. Using a wave-function model of nucleon structure, we fit single diffractive production as a function of excitation, and with the parameters so obtained predict the cross sections for double diffractive excitation.

I. INTRODUCTION

In hadronic diffractive production (DP) processes[1] of the type $a+b\to a^*+b^*$, we observe excited states $a^*(b^*)$ of $a(b)$, which manifest themselves as groups of hadrons with small relative velocities and the same quantum numbers (except possibly for spin-parity) as the ground state(s). The process is called diffractive because it involves no additive-quantum-number transfer and because such cross sections generally peak at small momentum transfer, t; we are concerned here with $0<-t\leq 1$ (GeV/c)^2. If one of the states a^* or b^* is the same as the corresponding incident state a or b, then the process is called single diffractive excitation (SDE); otherwise it is called double diffractive excitation (DDE). In all known cases, high-energy DP has the following characteristics:

(i) A strong correlation between the mass of the excited state and the slope of the forward peak $b = -(d/dt)\ln(d\sigma/dt)|_{t=0}$. When the larger of the two masses $m_a{}^*$ or $m_b{}^*$ is near threshold (e.g., in πN production, when $m^*\simeq m_\pi+m_N$) the slope b can be as much as a factor of two greater than the corresponding elastic slope. As m^* increases, the slope decreases, and seems consistent with attaining a constant asymptotic value of roughly half the elastic slope. The "asymptote" is reached at an excitation of $\sim 1-2$ GeV.

(ii) Near threshold (in the above sense) the DP cross section exhibits a richer t structure than elastic scattering, generally in the form of a sharp dip at $-t=0.25$ to 0.35 (GeV/c)^2. As m^* increases, this structure disappears.

(iii) The differential cross sections factorize among the various channels (to within the experimental error) in the sense that

$$d\sigma_{ab\to a^*b^*}=\frac{d\sigma_{ab\to ab^*}\,d\sigma_{ab\to a^*b}}{d\sigma_{ab\to ab}}\,. \qquad (1.1)$$

(This is the factorization relation which would follow from the exchange of a single Pomeron pole.)

In this paper we describe a simple model which accounts for the DP data in what we feel is a natural and transparent manner. We first apply the model to $NN\to(\pi N)N$ in order to determine certain parameters of the model. In the remainder of this paper we shall use the parameters we determined in SDE to calculate the corresponding DDE cross sections. We have not attempted to perform the analogous calculation for high-energy ($\pi\pi N$) SDE which then would be applied to the corresponding ($\pi\pi N$) DDE because, while the latter data are to some extent available,[2] the former are not; on the other hand, the (πN) SDE data were available to us in crude form,[3] but at present we have not seen any corresponding DDE data. In that sense, this paper serves as a prediction for (πN) DDE which we hope will spur the analysis and publication of such data.

We begin by describing our model and its application to SDE, and then discuss the extension to DDE. Motivated by current ideas about infinite binding of the constituents of hadronic matter, as well as by the desire to avoid inessential complications, we describe the internal structure of the hadrons and of their excited states as (bound) states in an infinite potential well. (Details of the well turn out to be unimportant.) The DP transition proceeds via constituent-constituent elastic scattering, as shown in Fig. 1, which can promote one or both constituents to excited states according to the overlap of the final and initial states. There is absorption in both incident and emergent channels (resulting from elastic rescattering) followed by (or during—again, this is not an essential detail) decay of the excited hadron(s) into the particles which are actually observed. The absorption is extremely important: Not only is it demanded by unitarity and by the strength of hadronic interactions, but without it the orthogonality of the eigenstates generated by a potential would cause the inelastic transition amplitudes to vanish at $t=0$. We restrict the present calculation to excitations with $l=0$, i.e., to non-spin-flip, or monopole transitions. While it would be both simple and natural to include higher multipole transitions within this kind of model, we feel there is value in determining to what extent the slope-mass relation and other salient features of SDE and DDE can be understood with monopole excitations only. There is some evidence,[4] based on a partial-wave analysis of $\pi N \to \pi\rho N$, in the $\pi\rho$ subsystem, that many of the features of DP hold for each partial wave in the excited-hadron subsystem. If this is so, then the effect must be explained without spin flip, as we have done here. To summarize, our model differs from many previous analyses of DP in two important ways: First, that we have used a specific form of the inelastic transition densities in impact-parameter space, thus keeping faith with the spirit of such quark-confinement models as the bag;[5] and second that (by contrast with Deck models[6] in which all natural-parity spin states of the subsystem are excited in a very specific dynamical way, or with "pure spin-flip" models[7]) we have restricted ourselves *only* to monopole transitions.

Once the excited-hadron state is diffractively produced, it must decay into the observed particles. The theoretical characterization of the decay amplitudes of bag-model states into physical multiparticle states is presently beyond the capability of infinite-confinement theories, and so we have chosen to take them as mass-dependent fitting parameters. An esthetic and physical requirement this approach imposes is that as the mass of the multiparticle excitation increases, the excitation should contain more of the higher states of the infinite-well basis.

Previous theoretical attempts to understand the transition of, say, a nucleon from its ground state to the diffractively excited state πN can conveniently be divided into two classes. In the first, the pion-exchange Deck effect[8] suggests virtual dissociation of a nucleon into an asymptotic pion and nucleon, with the pion scattering from the unexcited nucleon. (In nuclear or atomic physics this is simply direct breakup of a composite system.) Although the simple Deck model (without absorption) does not adequately account for the data,[9] recent work[6] has shown that inclusion of absorption (via rescattering of the produced and spectator nucleons) improves the fit. This model includes angular-momentum transfer, since in impact-parameter space the produced pion and nucleon scatter differently, at different points in space, from the unexcited nucleon. (However, many of the consequences of this model also hold partial wave by partial wave.) In the second class of theories, the dissociating nucleon goes directly into a state whose spin increases with the final mass $m_{\pi N}$. Using the empirical fact that the average s-channel helicity flip $\Delta\lambda$ increases with $m_{\pi N}$ as well as the known peripheral character[10] of diffractive dissociation, we see that these effects[7] generally broaden the forward peak because a particular impact parameter R (such as is effectively chosen by a peripheral process) contributes $J_{\Delta\lambda}(R\sqrt{-t})$ to the cross section, and $J_{\Delta\lambda\neq 0}$ contributes at larger $-t$ than J_0.

By its very nature, the Deck mechanism cannot accommodate resonance production; we note in this connection that the (quadrupole) $N(1688)$ is prominent in the data.[1] On the other hand, the "pure spin-flip" models[7] leave no room for monopole excitations such as the $N(1470)$. While our model implicitly includes the $N(1470)$ we omit (by choice) the $N(1688)$, but as we stated above, such resonances are easily included by a natural extension.

It is worth emphasizing that amplitudes with different helicity flip cannot interfere and therefore contribute incoherently to the differential cross section. It is just the coherent superposition of monopole transitions which produces the extreme steepness of near-threshold cross section by means of cancellations between the various terms.

The plan of the paper is as follows: In Sec. II we present the detailed theory. We follow this in Sec. III with a discussion of our fit to SDE of a nucleon into a pion-nucleus state. Using the parameters of SDE we discuss double excitation of the form $N+N\to(\pi N)+(\pi N)$ in Sec. IV.

II. THEORY

Where necessary we refer here, for definiteness, to transitions of a nucleon N to an excited state N^* which decays into a πN system. We also call the nucleon constituents quarks. The main ingredients of our theory are summarized graphically in Fig. 1. Note that in this figure the excited state N^*, labeled by the cross-hatched double line, can include the elastic state N, since the nucleon can decay into the (πN) state by virtue of its being off-shell. In this figure the double hatched ellipses represent absorption in the Sopkovich[11] sense, treated phenomenologically. The open square, f_{qq}, represents quark-quark scattering. Since absorption is simply the result of multiple scattering, f_{qq} is closely related to the absorption, as we see below. In addition, when the N^* is an excited state of the well, the horizontal ellipse measures the overlap with the ground state. Finally, as the figure indicates, we must expand the N^* state into (πN) states. This is done empirically by a fit to single excitation.

To make these comments more specific, we begin with the eikonal for elastic scattering. We assume the rescattering corrections for the excited states (or for the off-shell ground state) are identical to those for the incoming (ground-state) nucleons. Insofar as such cross sections have been measured in hadron-nucleus scattering experiments all "normal" hadronic states *do* have roughly the same cross sections. The Sopkovich prescription then consists simply of multiplication by the nucleon elastic S-matrix element. (We also could have absorbed an outgoing pion and nucleon independently on the other outgoing asymptotic state. Which of these is correct depends on the time scale for development of this asymptotic state from the N^*. Our investigation of this alternative possibility fortunately shows there is little empirical difference between these options.) We parametrize the nucleon-nucleon eikonal phase from experiment. A simple and reasonably accurate form is

$$i\chi(b)=\ln(1-de^{-b^2/a^2}), \qquad (2.1)$$

where b is the impact parameter, and d and a are taken from experiment. Given this eikonal phase, the elastic amplitude is

$$f(t)=-ip\int_0^\infty db\, bJ_0(b\sqrt{-t})(e^{i\chi}-1). \qquad (2.2)$$

In the Sopkovich prescription, rescattering and/or absorption is put in at each impact parameter through multiplication by $e^{i\chi(b)}$.

As we have stated above, the quark-quark interaction is not independent of this eikonal phase. Denote the single-quark ground-state density by $\rho_1(r)$ and let A be the number of quarks within a nucleon. (We consider only valence quarks here, so that densities for differing quarks are each normalized to unity. Moreover, all quarks have the same cross section, by assumption.) Then in the spirit of the Chou-Yang formalism[12] we may write

$$i\chi(b)=-\frac{A^2}{2}\sigma_{qq}^{\text{tot}}\int d^2b'\int_{-\infty}^{\infty}dz\int_{-\infty}^{\infty}dz'\rho_1(\vec{r}-\vec{r}\,')\rho_1(\vec{r}\,')$$
$$\equiv-\frac{A^2}{2}\sigma_{qq}^{\text{tot}}\int d^2b'\alpha_1(\vec{b}-\vec{b}')\alpha_1(\vec{b}'), \qquad (2.3)$$

where we use $\alpha_1(\vec{b})$ to denote the transverse density distribution. By two-dimensionally Fourier-transforming this quantity and comparing with the Fourier transform of Eq. (2.1) we can determine the parameters of this process. That is, define

$$\tilde{\alpha}_1(\vec{q})=\frac{1}{2\pi}\int d^2b\, e^{-i\vec{q}\cdot\vec{b}}\alpha_1(\vec{b}). \qquad (2.4)$$

Then

$$\int\frac{d^2b}{(2\pi)}e^{-i\vec{q}\cdot\vec{b}}\ln(1-de^{-b^2/a^2})=-\pi A^2\sigma_{qq}^{\text{tot}}\tilde{\alpha}_1{}^2(q). \qquad (2.5)$$

At $q=0$, the normalization of the densities makes $\tilde{\alpha}_1(0)=1/2\pi$ and Eq. (2.5) then yields

$$-A^2\sigma_{qq}^{\text{tot}}=-2\pi a^2\sum_{n=1}^{\infty}\frac{d^n}{n^2}=-\sigma_{NN}^{\text{tot}}\sum_{n=1}^{\infty}\frac{d^{n-1}}{n^2}. \qquad (2.6)$$

Using values for d and a taken from p-p elastic scattering and appropriate to the 43-mb pp total cross section at $\sqrt{s}=53$ GeV, namely[13] $d=0.724$ and $a=0.98$ fm, and taking $A=3$, Eq. (2.6) gives $\sigma_{qq}^{\text{tot}}\cong0.62$ fm^2, a reasonable value. (The same calculation for π-N scattering, using the experimentally determined values $d=0.574$, $a=0.88$ fm, and $A^2\to A_\pi A_p=6$ gives $\sigma_{qq}^{\text{tot}}=0.56$ fm^2.) By studying Eq. (2.5) for nonzero values of q and inserting (2.6) for $A^2\sigma_{qq}^{\text{tot}}$ we also determine $\tilde{\alpha}_1(q)$:

$$\tilde{\alpha}_1(q)=\frac{1}{2\pi}\left[\sum_{n=1}^{\infty}\frac{d^n}{n^2}\exp(-q^2a^2/4n)\Big/\sum_{n=1}^{\infty}\frac{d^n}{n^2}\right]^{1/2}. \qquad (2.7)$$

However, instead of using this (self-consistent) form explicitly, we chose to take the density functions from the ground-state wave functions of specific potential wells. This plan gives us the opportunity to test the sensitivity of our results to different choices of potential well. While these potential wells will not as a result be precisely consistent with Eq. (2.1) for the eikonal function (a function which is itself an approximation when compared to pp-scattering data), the insensitivity of our results to the choice of potential well convinces us that this deficiency is unimportant. Moreover, we directly compared the "experimental" form factor, Eq. (2.7), with those derived from potential wells and found little differ-

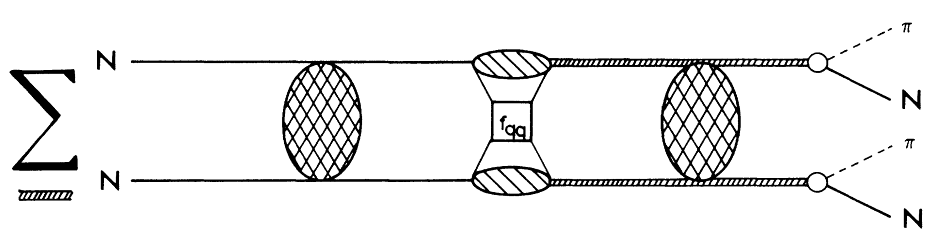

FIG. 1. Diagrammatic representation of the impulse approximation with absorptive corrections for diffractive production of excited states of nucleons.

ence out to $q^2 = 1$ (GeV/c)^2, which is the important region for the DP calculation.

We next study the transitions. These can be handled in a compact and convenient way by adding to the ground-state c-number density $\alpha_1(\vec{b})$ an operator $\alpha_{tr}^{op}(\vec{b})$ which induces transitions. This operator only connects different states: Thus if we think of $\alpha_1(\vec{b})$ as the ground-state expectation of the quark-density operator, then, $\alpha_{tr}^{op}(\vec{b})$ is the fluctuating part of the quark density. The matrix elements of α_{tr}^{op} are just the b-space overlaps of the potential-well wave functions $\phi_n(\vec{r})$; that is $[\alpha_{11}(\vec{b}) \equiv \alpha_1(\vec{b})]$:

$$\langle n|\alpha_{tr}^{op}|1\rangle = \int_{-\infty}^{\infty} dz\, \phi_n(r)\phi_1^*(r) \equiv \alpha_{n1}(\vec{b})\,. \tag{2.8}$$

The eikonal function then takes the form (2.3) with $\alpha_{11} \to \alpha_{11} + \alpha_{tr}^{op}$; Eq. (2.2) stands with the understanding that the matrix element between appropriate initial and final states is to be taken. Finally, in accordance with the idea that the transition should be treated in lowest order we expand the amplitude to lowest order in α_{n1}, $n \neq 1$. [Even integrated over all $N\pi$ masses, the total cross section for the process $N+N \to (N\pi)+N$ is about 1% of the total N-N cross section. However, the sum of all diffractive dissociation channels may be considerably larger, and the reader should be aware of an alternate point of view[14] in which a lowest-order expansion may not be appropriate.]

The matrix element computed in this way represents the transition of one or both of the nucleons to excited states N_n^* of the infinite well. We must decompose these states (including the ground state) into the $N\pi$ (say) system of mass m^* observed in an experiment. Thus, we require mixing coefficients $c_n(m^*)$ (fitting parameters),

$$|N\pi\rangle = \sum_{i=1} c_i(m^*)\,|N_i^*\rangle\,. \tag{2.9}$$

Using (2.9), (2.8), and expanding (2.2) to lowest order in α_{n1} we have for the single-excitation amplitude

$$\langle (N\pi)_A N_B|f(t)|N_A N_B\rangle = -ip\int_0^{\infty} db\, bJ_0(b\sqrt{-t})\left[c_1(m_A^*)(e^{i\chi(b)}-1) - \frac{AB}{2}\sigma_{qq}^{tot}e^{i\chi(b)}\sum_{i=2} c_i(m_A^*)\int d^2b'\,\alpha_{i1}(\vec{b}-\vec{b}')\alpha_{11}(\vec{b}')\right], \tag{2.10}$$

and for the double-excitation amplitude (note that here, consistency requires keeping some *second-order* terms in α_{tr}^{op})

$$\langle (N\pi)_A (N\pi)_B|f(t)|N_A N_B\rangle$$

$$= -ip\int_0^{\infty} db\, bJ_0(b\sqrt{-t})\Big[c_1(m_A^*)c_1(m_B^*)(e^{i\chi(b)}-1) - \frac{AB}{2}\sigma_{qq}^{tot}e^{i\chi(b)}\sum_{i,j=1} c_i(m_A^*)c_j(m_B^*)(1-\delta_{i+j,2})\int d^2b'\,\alpha_{i1}(\vec{b}-\vec{b}')\alpha_{j1}(\vec{b}')$$

$$+ e^{i\chi(b)}\sum_{i,j=2} c_i(m_A^*)c_j(m_B^*)\left(\frac{AB}{2}\sigma_{qq}^{tot}\int d^2b'\,\alpha_{i1}(\vec{b}-\vec{b}')\alpha_{11}(\vec{b}')\right)^2\Big]. \tag{2.11}$$

In these expressions we have for convenience labeled the nucleons with A and B; A and B also denote their respective number of constituents. The eikonal phase $i\chi(b)$ is given by Eq. (2.1); we remind the reader that it contains no transition matrix elements. Note too that the elastic term in Eq. (2.10) and (2.11) is also treated (more precisely) by means of the phenomenological elastic behavior of Eq. (2.1). Only in those terms where there is at least one transition to a potential-well excited state is it simpler to use $\alpha_{11}(\vec{b})$.

III. FIT TO SINGLE DIFFRACTIVE EXCITATION

We here treat the $\sqrt{s} = 53$ GeV CERN ISR data[3] for the process $p+p \to p+(n\pi^+)$. The data were taken in six mass bins for $m_{n\pi^+}$, from 1.15 to 3 GeV/c^2 and the reaction is measured from $t \simeq -0.1$ (GeV)^2 to $\simeq -0.8$ (GeV)^2. This data contains both resonant and nonresonant (in the π^+n state) contributions.[3] By far the clearest resonant signal seen is the $N(1688)$, which may account for 20% of the cross section. The $N(1688)$ obviously is not an $l=0$ excitation, so we must take this as a basic uncertainty of our results at the 20% level, especially in the region around 1688 MeV/c^2.

In an effort to test the sensitivity of our results to the choice of potential well, we used both an infinite square well of radius R as well as an (infinite) harmonic oscillator, with strength parameter chosen so that the ground-state rms radius matches the corresponding radius for the square well. The wave functions and rms radii are

$$\left.\begin{aligned}\phi_n(r) &= \left(\frac{2}{R}\right)^{1/2}\frac{1}{r}\sin\frac{n\pi r}{R}\,, &(3.1\text{a})\\ \langle r_n{}^2\rangle &= \frac{R^2}{3}\left[1-\frac{3}{2}\frac{1}{n^2\pi^2}\right] &(3.1\text{b})\end{aligned}\right\}\text{(square well)}$$

$$\left.\begin{aligned}\phi_1(r) &= N_1\exp(-r^2/2c^2)\,,\\ \phi_2(r) &= N_2(1-\tfrac{2}{3}r^2/c^2)\exp(-r^2/2c^2)\,, &(3.2\text{a})\\ \langle r_n{}^2\rangle &= (n+\tfrac{3}{2})c^2 &(3.2\text{b})\end{aligned}\right\}\text{(harmonic oscillator).}$$

The equality of $\langle r_1{}^2\rangle$ for (3.1b) and (3.2b) is guaranteed by the choice $c = 0.43R$. The square well is particularly intriguing not only for its analytic simplicity but also because of the insensitivity of $\langle r_n{}^2\rangle$ to n. This means all excited states have the same radii, in accordance with the approximate equality of all hadronic cross sections.

Our results were insensitive to the choice of potential. With either potential, we fit the peripheral structure of SDE better with the value $R = 1$ fm, rather than $R = 1.5$ fm which would be required by a fit of the ground state to the proton rms charge radius. The "true" form factor, Eq. (2.7), which was determined from the experimental eikonal function, has the property that while it gives the correct proton charge radius, it falls much more slowly at large q^2 than those we used in our calculation. Thus our use of a smaller radius in the transition form factors is a compromise.

Our procedure is, given the various overlap functions, to fit the $c_i(m_{\pi^+n})$ to the data according to Eq. (2.10) in a least-squares sense, reading the data from the graphs of Ref. 3. We included up to four excited-state amplitudes; for either the square well or harmonic oscillator the quality of the fits (χ^2/degree of freedom) decreased with more than two parameters (one excited state plus the quasielastic term). Table I lists the values of the parameters as determined from these fits.

The astute reader will notice that in Eq. (2.10) only $c_1(m^*)$ and the combination $(AB/2)\sigma_{qq}^{\text{tot}}c_i(m^*)$ $(i \neq 1)$ appear. For Table I we took the factor $(AB/2)\sigma_{qq}^{\text{tot}}$ to be 2.78 fm^2, according to Eq. (2.6), but this means there is some uncertainty in c_2, according to uncertainty in $(AB/2)\sigma_{qq}^{\text{tot}}$.

TABLE I. Values of mixing coefficients $c_i(m^*)$ (see text) extracted from fit to single diffractive excitation.

Mass bin (GeV/c^2)	Square well c_1	Square well c_2	Harmonic oscillator c_1	Harmonic oscillator c_2
No. 1: 1.15–1.32	0.0827	−0.128	0.0828	−0.127
No. 2: 1.32–1.44	0.0941	0.0477	0.0939	0.0391
No. 3: 1.44–1.56	0.0740	0.103	0.0738	0.0939
No. 4: 1.56–1.80	0.0856	0.125	0.0854	0.116
No. 5: 1.80–2.4	0.0558	0.108	0.0557	0.100
No. 6: 2.4–3.0	0.0200	0.0694	0.0198	0.0612

The parameters c_1 and c_2 have fairly smooth and reasonable mass dependences, c_1 falling and c_2 exhibiting a peak. The mass bin 1.56–1.80 exhibits a jump in c_1 which may result from the contribution of the quadrupole transition to the $N(1688)$ resonance. If this resonance affects the size of $d\sigma/dt$ in this mass bin but not its shape, then c_1 will be more sensitive to the subtraction of the $N(1688)$ than will c_2; the behavior of the c_i thus could become even smoother with mass if the resonance contribution were subtracted from the data.

Figure 2 shows the fit for the six mass bins given in Ref. 3; this fit is that of the square well. The harmonic-oscillator fit is very similar with minor differences for $t \gtrsim 0.8$ (GeV/c)^2 (dashed curves).

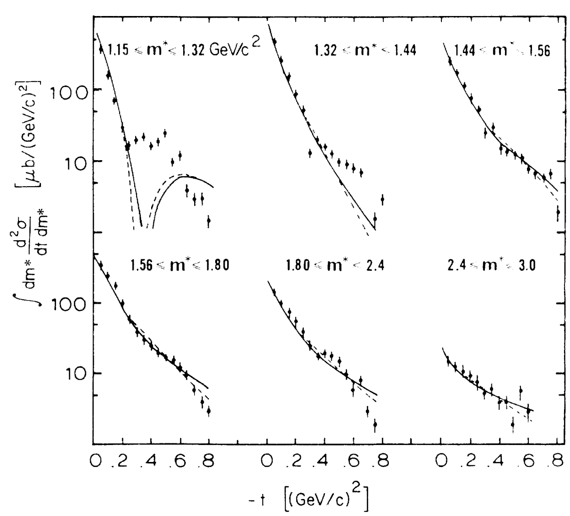

FIG. 2. Data from Ref. 3 for single diffractive production of $(n\pi^+)$ at $\sqrt{s} = 53$ GeV in pp collisions, together with theoretical fits using the theory described in the text.

IV. DOUBLE DIFFRACTIVE EXCITATION

Equation (2.11) makes clear that we must distinguish between the factors $(AB/2)\sigma_{qq}^{tot}$ and c_2. For example, in Eq. (2.11) the direct term between $c_2(m_A^*)$ and $c_2(m_B^*)$ is proportional to

$$\tfrac{1}{2}AB\sigma_{qq}^{tot}c_2(m_A^*)c_2(m_B^*) = (\tfrac{1}{2}AB\sigma_{qq}^{tot})^{-1}[\tfrac{1}{2}AB\sigma_{qq}^{tot}c_2(m_A^*)][\tfrac{1}{2}AB\sigma_{qq}^{tot}c_2(m_B^*)]\ .$$

From Eq. (2.6) we take the value $\frac{1}{2}AB\sigma_{qq}^{tot}=2.78$ fm^2 in nucleon-nucleon collisions. Given this result and the parameters given in Sec. III, the cross section for DDE is completely determined.

The overlap integrals in Eq. (2.11) are far simpler to perform numerically when the transition densities arise from harmonic oscillators since in this case we have analytic expressions for the $\alpha_{n1}(b)$. The difference in difficulty is so large that we had to forego the square-well calculation. We calculated the cross sections for DDE $[p+p \to (N\pi)+(N\pi)]$ in 21 mass bins corresponding to the six SDE mass bins of Ref. 3. We graph selected cross sections in Fig. 3 and give some of the salient features in Table II; regularities become apparent. Table II lists the values of the cross sections $d\sigma/dt$ at $t=0$ and the slopes as measured from $t=0$ to $t=-0.1$ $(GeV/c)^2$. In this table the mass bins are labeled as in Table I. Additionally, the location and type of structure in t is indicated.

One should note the extremely large slope for the 1-1 DDE mass bin. The slope shows a systematic decrease as one or both of the $(N\pi)$ masses increases. In the very highest mass bins, where the broad dips appear, the cross sections actually exhibit very broad *maxima* at values of $-t$ from 0.5 to 1 $(GeV/c)^2$. The cross sections are also quite small at these large mass bins. Although not indicated in the table, the dip structure also is systematically less sharp as the masses increase. The features described above are qualitatively just like SDE.

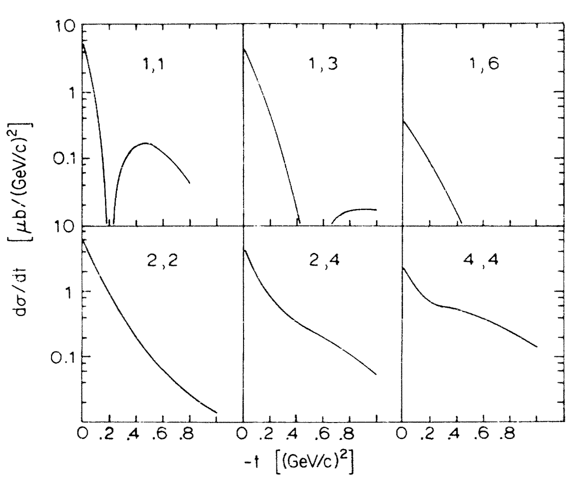

FIG. 3. Predicted differential cross sections for selected mass bins in double diffractive production, obtained as described in the text.

Table II also shows a rise in $d\sigma/dt$ at $t=0$ when one of the two excited masses is in mass bin 4. This is the mass interval covering the $N(1688)$, and the reason for the rise is connected with this state. Even though the $N(1688)$ was formally excluded by our restriction to monopole excitations, it is reflected in our parameters for this mass bin through the fit to SDE.

Another experimentally accessible feature of DDE is factorization. In the sense implied by the exchange of a simple Pomeron pole, factorization for diffractive excitation means

$$R(t)\equiv\frac{d\sigma(p+p\to p+B^*)d\sigma(p+p\to A^*+p)}{d\sigma(p+p\to p+p)d\sigma(p+p\to A^*+B^*)}=1\ . \tag{4.1}$$

This relation has been tested[15] at $\sqrt{s}=45$ GeV, where A^* is a $(p\pi^+\pi^-)$ state of masses summed from 1.3 to 1.85 GeV/c^2 [dominated by the $N(1688)$] and B^* is any nonelastic diffractive state, i.e., it is inclusively measured. In particular for three t regions from 0.15 to 0.525 $(GeV/c)^2$, $R(t)$ was found to be unity to within about 30%–40%. In this experiment one should

TABLE II. Predicted forward differential cross sections $[\mu b/(GeV/c)^2]$, slopes $[(GeV/c)^{-2}]$, and positions $[(GeV/c)^2]$ and characters of dips (if any).

Mass bin	$d\sigma/dt_{t=0}$	Slope	Dip in t
1-1	5.4×10^{-2}	20.7	−0.2
1-2	7.5×10^{-2}	13.6	−0.4
1-3	4.8×10^{-2}	11.3	−0.5
1-4	6.4×10^{-2}	11.1	−0.5
1-5	2.8×10^{-2}	10.0	−0.55
1-6	3.7×10^{-3}	7.3	−0.65
2-2	6.5×10^{-2}	10.9	
2-3	3.3×10^{-2}	9.5	
2-4	4.3×10^{-2}	9.4	
2-5	1.6×10^{-2}	8.6	
2-6	1.4×10^{-3}	5.8	
3-3	1.4×10^{-2}	8.4	
3-4	1.8×10^{-2}	8.3	
3-5	6.3×10^{-3}	7.5	
3-6	3.6×10^{-4}	4.1	−0.1 (broad)
4-4	2.4×10^{-2}	8.1	
4-5	8.0×10^{-3}	7.4	
4-6	4.3×10^{-4}	3.9	−0.1 (broad)
5-5	2.5×10^{-3}	6.5	−0.2 (broad)
5-6	$9\ \times10^{-5}$	1.9	−0.05 (broad)
6-6	10^{-6}	2.6	−0.1 (broad)

recognize first that because the cross sections fall with the mass of B^* one is testing factorization for relatively small masses, and second that in the reactions so far tested deep dips have not been in evidence.

We tested factorization according to the generalization of Eq. (4.1), namely,

$$R_{ij}(t) = \frac{\{d\sigma[p+p\to(N\pi)_i+(N\pi)_j]\}^2}{d\sigma[p+p\to(N\pi)_i+(N\pi)_i]\,d\sigma[p+p\to(N\pi)_j+(N\pi)_j]}\,. \tag{4.2}$$

Here the subscript labels the mass bin; in particular the subscript 0 labels the elastic state, $(N\pi)_0\equiv p$. Thus the subscripts run from 0 to 6. [The factorization relation of Eq. (4.1) may be derived from linear combinations of (4.2).] Table III lists these factorization ratios. Several conclusions may be drawn from this table. First, in view of the wide variation of the cross sections themselves it may at first be surprising that factorization works so well. When it does work, it is because[16] of the effective dominance of c_1 over c_2 (or vice versa) in the cross section: With a single parameter, factorization would be exact in our theory. We then expect factorization can only fail where the two parameters give comparable contributions. This is clearly reflected in Table III. For example mass bin No. 1 is the bin where the steep forward slope is a result of interference between the two pieces. All the $R_{ij}(t)$, where either i or $j=1$, are far from unity (but note, not orders of magnitude different from unity). This is also reflected in mass bin No. 6,

TABLE III. Predicted factorization ratios at various values of t in $(\mathrm{GeV}/c)^2$.

ij	$R(t=0)$	$R(-0.1)$	$R(-0.2)$	$R(-0.3)$	$R(-0.4)$
01	1.3	1.5	1.8	2.9	24.6
02	1.0	1.0	1.0	1.0	1.1
03	1.3	1.4	1.4	1.5	1.5
04	1.4	1.5	1.5	1.6	1.6
05	2.1	2.3	2.3	2.2	2.2
06	48.3	115	670	27.6	10.1
12	1.6	1.9	2.5	4.4	44.7
13	3.0	4.0	5.8	11.4	138
14	3.2	4.4	6.4	12.7	154
15	5.7	8.0	11.8	23	277
16	240	755	6×10^3	509	2.3×10^3
23	1.2	1.2	1.2	1.2	1.2
24	1.2	1.2	1.2	1.2	1.2
25	1.6	1.7	1.7	1.6	1.6
26	29.5	67.5	391	16.3	6.0
34	1.0	1.0	1.0	1.0	1.0
35	1.1	1.1	1.1	1.1	1.1
36	3.5	19.9	122	6.0	2.6
45	1.1	1.1	1.1	1.1	1.0
46	7.3	1.6	108	5.5	2.4
56	2.8	6.5	52.8	3.4	1.7

(and to a lesser extent in No. 5), where the c_1 and c_2 terms are again comparable.

The experiment of Ref. 15 does not test factorization in the regions where our results state it fails. We believe our predictions are consistent with experiment, and suggest that an experimental test of factorization as in Table III would be most interesting.

Note added in proof. We would like to draw the reader's attention to a related paper by Hama,[17] which we encountered recently.

---

*Work supported in part by the National Science Foundation.

[1]For some recent reviews see M. Derrick, in *Particles and Fields-1975*, proceedings of the Meeting of the Division of Particles and Fields of the APS, Seattle, edited by H. J. Lubatti and P. M. Mockett (Univ. of Washington, Seattle, 1976); D. Leith, Lectures at Canadian IPP International Summer School, Montreal, June, 1975, SLAC Report No. SLAC-PUB-1646 (unpublished); H. Miettinen, in *High Energy Physics*, proceedings of the European Physical Society International Conference, Palermo, 1975, edited by A. Zichichi (Editrice Compositori, Bologna, 1976), p. 731.

[2]M. Cavalli-Sforza *et al.*, papers No. 63-19, 20, 21 submitted to the European Physics Society International Conference on High Energy Physics, Palermo, June, 1975 (unpublished).

[3]E. Nagy *et al.*, CERN-Hamburg-Orsay-Vienna collaboration, Paper No. 489 submitted to the XVII International Conference on High Energy Physics, London, July, 1974 (unpublished).

[4]Yu. Antipov *et al.*, Nucl. Phys. B63, 153 (1973).

[5]See K. Johnson, Acta Phys. Pol. B6, 856 (1975) and references contained therein.

[6]E. Berger and P. Pirilä, Phys. Rev. D 12, 3448 (1975). These authors do point out that the various phenomenological effects occur in their model partial wave by partial wave.

[7]N. Sakai and J. White, Nucl. Phys. B59, 511 (1972); S. Humble, *ibid.* B76, 137 (1974) and B86, 285 (1975).

[8]S. Pokorski and H. Satz, Nucl. Phys. B19, 113 (1970) and references contained therein.

[9]M. Miettinen and P. Pirilä, Phys. Lett. 40B, 127 (1972).

[10]L. Caneschi *et al.*, Phys. Lett. 56B, 359 (1975).

[11]N. Sopkovich, Nuovo Cimento 26, 186 (1962).

[12]T. Chou and C. N. Yang, in *High Energy Physics and Nuclear Structure*, edited by C. Alexander (North-Holland, Amsterdam, 1967).

[13]G. Barbiellini *et al.*, Phys. Lett. 39B, 663 (1972); R. J. N. Phillips and V. Barger, *ibid.* 46B, 412 (1973). In the latter reference we found it necessary for this energy to use (notation of Phillips and Barger)

$\frac{1}{2}D+a' \ln s=5.4$ and $\sqrt{A}=8.8$.

[14]K. Fiałkowski and H. Miettinen, CERN Report No. TH. 2057; P. Camillo and P. Fishbane, Phys. Rev. D 13, 740 (1976).

[15]R. Webb *et al.*, Phys. Lett. 55B, 336 (1975).

[16]P. Fishbane and J. Trefil, Phys. Rev. D 10, 3005 (1974).

[17]Y. Hama, Phys. Rev. D 6, 3306 (1972).